

Gaussian Filter-Based Feature Extraction with Machine Learning Classifiers for Automated Classification of Synthetic Retinal Fundus Images

Dr P Anbarasi¹, Dr R Ramprasad², Dr.P.Sasikala³, Dr P Radhika⁴, Mrs C Rajapriya⁵

Assistant Professor & Head, Department of Computer Science, Sri Muthukumaran Arts and Science College,
Chennai, India¹

Assistant Professor & Head, Department of Computer Applications, Sri Muthukumaran Arts and Science College,
Chennai, India²

Professor & Principal, Jaya Women's College (Arts & Science), Chennai, India³

Assistant Professor, Department of Computer Applications, Sri Muthukumaran Arts and Science College,
Chennai, India⁴

Assistant Professor, Department of Computer Science, Sri Muthukumaran Arts and Science College, Chennai, India⁵

ABSTRACT: The Retinal Fundus Image is a very non-invasive and accessible diagnostic tool, and can offer a lot of information for the diagnosis of many systemic and ocular conditions, including diabetic retinopathy, glaucoma, age related macular degeneration, and hypertensive retinopathy. Automated classification of retinal fundus images with high accuracy is clinically important for early detection of disease and population scale screening. Additionally, synthetic retinal fundus data generated by computational simulation can be used instead of patient imaging data for algorithm development and benchmarking, and can be a privacy-preserving and reproducible resource. This research aims at evaluating the performance of Gaussian Filter (GF) based image feature extraction and six machine learning classifiers, namely instance-based, discriminant and tree-based, for automatic classification of synthetic retinal fundus images of the Kaggle Synthetic Retinal Fundus Images dataset. The dataset (Synthetic Retinal Fundus Images) from Kaggle (<https://www.kaggle.com/datasets/taanii/synthetic-retinal-fundus-images>) was used for the evaluation. All images have been pre-processed with Gaussian filter prior to feature extraction. The classifiers used were: Radius Neighbors, Nearest Centroid (instance-based); Fisher's Linear Discriminant, Regularized Discriminant (discriminant); Decision Tree CART, ID3 Decision Tree (tree-based). The accuracy, precision, recall, ROC area, PRC area and training time were used for the evaluation in Weka 3.8 framework. The best overall performance was achieved with GF+Decision Tree (CART) which had an accuracy, precision, recall, ROC area and PRC area of 0.89, 0.88, 0.87, 0.95, and 0.93 respectively and a training time of 5.89 seconds. The best efficiency (2.34 sec) and a good accuracy (85.29 %) and ROC (0.91) was obtained by GF+Regularized Discriminant. The lowest accuracy (80.39% and 80.35% respectively) was provided by the GF+Fisher's Linear Discriminant and the GF+ID3 Decision Tree. Gaussian Filter + CART Decision Tree performs best overall while Gaussian Filter + Regularized Discriminant is the most efficient algorithm to compute. The Gaussian filter pipeline offers an easy-to-interpret, clinically feasible and lightweight approach to automated retinal image classification.

KEYWORDS: Gaussian Filter, CART, glaucoma, retinal fundus, diabetic.

I. INTRODUCTION

Retinal fundus photography provides an indirect, non-invasive assessment of the microvasculature of the eye and is a useful diagnostic tool for many diseases of both the eye and the body. Diabetic retinopathy (DR), glaucoma, age-related macular degeneration (AMD) and hypertensive retinopathy are characterized by changes that can be seen in the retinal fundus, and are the major causes of preventable visual impairment and blindness in the world [1]. The impact of the visual impairment due to retinal disease is enormous, diabetic retinopathy alone causing about one-third of all cases of new onset vision loss in young to middle age adults.

The promise of machine learning and computer vision for automated classification of retinal fundus images is a game-changing opportunity to conduct retinal disease screening at population level in primary care, community and low resource settings which is not possible by specialist ophthalmologists. Patient privacy regulations, the expense of expert annotation and the scarcity of advanced disease stage cases limit the size, well-annotated nature, and availability of screening population retinal imaging data for use in developing and validating automated retinal image classification algorithms.

Synthetic datasets of retinal images have been created by computational simulation of retinal anatomy and pathology, offering a reproducible and privacy-preserving alternative for the development and benchmarking of algorithms which can be scaled to increase the number of images [3]. Synthetic datasets enable systematic evaluation of classification pipelines with known distribution without the variation associated with real clinical retinal imaging datasets, or class imbalance. In those cases, a standardized set of images are provided for testing and evaluating automated retinal classification algorithms in a standardized manner, known as the Synthetic Retinal Fundus Images dataset on Kaggle.

The Gaussian Filter is a linear filter for image smoothing that convolves the image with a Gaussian filter and reduces the high-frequency noise while maintaining low-frequency information in the image, including information related to the diagnosis of retinal diseases for classification of retinal diseases, such as retinal vessel boundaries, boundaries of the optic disc, and boundaries of lesions. The objective of this work is to evaluate the performance of the Gaussian filter-based features extraction combining six classifiers from three different algorithmic families (instance based, discriminant, tree based) for the identification of best performance of the GF-classifier configuration in the context of automatic classification of retinal fundus images from the Synthetic Retinal Fundus Images dataset.

Paper is organized as follows. Section II shows the related works. Materials and methods are given in Section III. Section IV presents experimental results showing results of images tested. Finally, Section V presents conclusion.

II. RELATED WORK

This chapter will deal with epidemiology and clinical background of Diabetic retinopathy (DR). It is the most prevalent microvascular complication of diabetes mellitus (DM) and is a major preventable cause of visual impairment and blindness in working age adults throughout the world. Lee et al. [1] performed a comprehensive epidemiological study of DR, diabetic macular edema (DME) and vision loss and found that approximately 1 in 3 individuals with diabetes worldwide have DR and approximately 1 in 30 individuals have diabetic macular edema (DME), which in turn leaves approximately 10 million or more individuals at risk for vision loss from DR. Results of this study have shown that the burden of DR related visual impairment will be greatly increased in the near future if the prevalence of diabetes continues to increase, and new clinical systems which can be scaled and automated are desperately needed.

Salz and Witkin [2] studied various imaging modalities in DR, including fundus photography, fluorescein angiography, optical coherence tomography, and found that the hierarchy of retinal imaging tools and fundus as the first-line imaging modality for DR screening programs has been set. They provided context for the use of imaging protocols in automated fundus image classification algorithms (e.g., the Gaussian filter-based method in this study) in a clinical setting. Several methodological generations of automated detection of DR have been comprehensively reviewed. Automated Diabetic Retina Detection: Review: A number of methodological generations of automated detection of DR have been reviewed. Salamat et al. [3] in a systematic review, discussed classical image processing techniques, machine learning techniques and early deep learning techniques for DR lesion detection, segmentation, and DR grading in retinal images.

Chaturvedi et al. [4] conducted a systematic review on the progress of computer-aided diagnosis (CAD) for DR from the early detection of DR lesions to feature engineered machine learning classifiers to end-to-end deep learning architectures. The present study is directly inspired by their survey where they found that the difference in performance between the traditional machine learning and deep learning algorithms is minimal when using high quality feature descriptors and classical pipelines. Saha et al. [5] explored the particular difficulty with the fundus image registration technique and its use in automated analysis of progression of diabetic retinopathy disease. They discussed it in Biomedical Signal Processing and Control and found that the quality of image-level features descriptors, like image representations derived from a Gaussian filter, is crucial to all downstream automated DR analysis tasks, including image registration and tracking of a disease over time. 3.

The first and most critical signs of DR are red lesions (microaneurysms and dot haemorrhages) which occur before any clinical visual symptoms and are the main reason for referral for DR screening. Biyani and Patre [6] performed in-depth survey on the algorithms used for red lesion detection in DR, which included both morphological filtering and matched filter methods, ensemble classifiers and early CNN based red lesion detectors. They have published their review in Biomedicine and Pharmacotherapy where they set up the performance benchmarks and methodological development for red lesion detection in retinal fundus images, emphasizing local texture descriptors and neighbourhood-based classification as the most promising classical approaches to discriminate between real red lesions and segments of blood vessels and others interfering structures. Dashtbozorg et al. [7] introduced a major breakthrough in the methodology of microaneurysm detection which involves the features of Local Convergence Index (LCI) of the retina.

Eftekhari et al. [8] introduced a two-stage convolutional neural network to identify microaneurysms in fundus images in Biomedical Engineering Online. They found that by adding a candidate generation step, which involves morphological preprocessing that identifies potential locations of microaneurysms, and a CNN-based classification step, which classifies the candidates as microaneurysms or false positive, good performance can be obtained. The severe class imbalance problem common to microaneurysm detection problems was solved in this two-step method, by increasing sensitivity at clinically acceptable false positive rate, in a microaneurysm detection problem where true positive lesions are sparse against millions of non-lesion pixels. Budak et al. [12] proposed a novel CNN-based framework to combine reinforcement sample learning for detecting microaneurysm in Health Information Science and Systems. Their approach was based on the fundamental issue of limited annotated training data in retinal imaging as they added a reinforcement learning element that adaptively chose the most informative training samples for CNN fine-tuning to achieve a better generalization performance than the standard supervised training on small retinal datasets. In cases where large annotated datasets are scarce, they found that data-efficient deep learning techniques can be competitive in detecting microaneurysms, a key requirement for clinical deployment scenarios. 5. Classical Machine Learning and Signal Processing Methods for Microaneurysm Detection, though deep learning has become the mainstream approach for microaneurysm detection, classical machine learning and signal processing are also viable and explainable methods for microaneurysm detection. Zhou et al. [9] presented their research in IEEE Access which introduced an automatic microaneurysm detection method based on sparse principal component analysis (sPCA) and unsupervised classification. They used a sparse representation approach in decomposing retinal fundus images and they identified candidates of microaneurysm as a sparse component of the image with characteristic morphological profiles. One of their key benefits is that they are unsupervised – that is, they do not require any hand-annotated training data. Computerized Medical Imaging and Graphics published an article by Wu et al. [10] which is an automatic detection system for microaneurysms in retinal fundus images. They used multi-scale Gaussian filtering (a very close pre-processing to the one used in the current study), morphological candidate extraction and feature-based classification. The variable size of microaneurysms from patient to patient and imaging conditions, motivated the use of multi-scale Gaussian filtering in order to better preserve the spatial frequency content of the microaneurysm structures than if the processing was carried out at a single scale. Wang et al. [11] introduced a completely different signal processing technique to localize microaneurysms in fundus images using singular spectrum analysis (SSA) in IEEE Transactions on Biomedical Engineering. They used the SSA for their retinal image signals and separated periodical components that were associated with the intensity profiles of the microaneurysms from the background retinal texture. This spectral decomposition technique show that signal processing techniques are able to extract frequency signatures specific to the microaneurysm, which are not available in the spatial domain feature extractors, hence offering complementary detection method to morphological and CNN-based methods. In [13] Habib et al. proposed a Microaneurysm Detection Framework (MicroF) in the context of retinal images using an ensemble-Classifier technique, as part of the Informatics in Medicine Unlocked research paper.

The Texture Feature Descriptors for Retinal Image Classification part of the section is addressed. In this section, the Texture Feature Descriptors for Retinal Image Classification is discussed. Retinal fundus image classification has employed several local texture descriptors for their characteristic textural properties related to the pathological structure of the retinas, as feature extracting techniques. In the Journal of Digital Imaging, Derwin et al. [14] presented a secondary observer (SO) system for detecting microaneurysm (MA) in fundus images that is based on texture descriptors. Their system relies on the use of texture features: Local Binary Pattern (LBP), Gray-Level Co-occurrence Matrix (GLCM) and Gabor filter to identify candidate microaneurysm regions, and they found that the

multi-descriptor texture feature fusion is better than the single-descriptor classification to differentiate the microaneurysm regions from the vessel segments and hard exudates.

The fusion approach of these texture descriptors proved to be useful for retinal lesion classification, as such high accuracy was achieved in classification of the candidates for microaneurysm using good synergy between local structural patterns of LBP, second order statistical relationships of GLCM and frequency selective responses of Gabor, motivating a Gaussian filtering feature extraction approach, which was evaluated in the present study. 7. The most recent and detailed review was conducted by Mayya et al. [15] who gave a systematic review of automated detection of microaneurysm for early diagnosis of DR in Computer Methods and Programs in Biomedicine Update. On a suite of standard retinal datasets such as DIARETDB1, MESSIDOR and the Retinopathy Online Challenge, they investigated all the possible approaches from the morphological detectors and handcrafted feature classifiers to deep convolutional neural networks.

III. METHODOLOGY

3.1 Dataset

The dataset of synthetic Retinal Fundus Images was retrieved from Kaggle [16]. The dataset is comprised of the calculated retinal fundus images of different types of normal and pathological retinal images. Patient identifiers are removed from all images and they are freely available for algorithm development, and freely available for synthetic generation to be used for benchmarking. The experiments that were implemented and executed were realized and performed in the Weka 3.8 machine learning workbench [6].

3.2 Gaussian filter

The Gaussian filter convolves each of the input images with a 2D Gaussian kernel:

$$.G(x, y) = (1 / 2\pi\sigma^2) \cdot \exp-(x^2 + y^2) / 2\sigma^2$$

The amount of smoothing is determined by the value of σ , the smoothing radius. The Gaussian filter has the effect of attenuating the acquisition noise in the high frequencies while preserving low frequencies of structures which are the major feature sources for retinal disease classification: boundaries of retinal vessels, margins of the optical disc, and edges of lesions [4,10]. All images were then resized to 224×224 pixels and normalized to [0, 1] for feature extraction.

3.3 Machine Learning Classifiers

To test the classifiers, three families of classifiers were used, which were:

- Instance-Based Classifiers:
 - ✓ Radius Neighbors: Dynamically variable neighbourhood size with fixed Gaussian feature space radius – assigns a class to each test image based on the majority class of all training images in a local neighbourhood, which is defined by a fixed Gaussian feature space radius and dynamically varying neighbourhood size according to the variations in local feature density.
 - ✓ Nearest Centroid: Assign each test image to the class of the centroid of the class that it in Gaussim feature space. The class in Gaussim feature space is represented by the centroid of the feature vectors in the training set.
- Discriminant Classifiers:
 - ✓ Fisher's Linear Discriminant: Project Gaussian features onto the axis with the largest Fisher criterion (between-class to within-class variance ratio) to get a linear decision boundary optimized for normally distributed features.
 - ✓ Regularized Discriminant: Smoothes the LDA and QDA solutions by computing the convex combination of these two solutions to use when the number of features for a Gaussian distribution is very large compared to the number of samples for each class, so that the covariance can be properly estimated in the classes.
- Tree-Based Classifiers:
 - ✓ Decision Tree CART: Creates a binary decision tree, using gini impurity as a splitting criterion and cost-complexity pruning to avoid overfitting, gaussian features. Generates understandable rules for thresholds.

- ✓ ID3 Decision Tree: Builds decision tree using information gain (entropy reduction) to partition nodes and chooses Gaussian feature split that has highest class purity. Different splitting criterion other than Gini index used by CART.

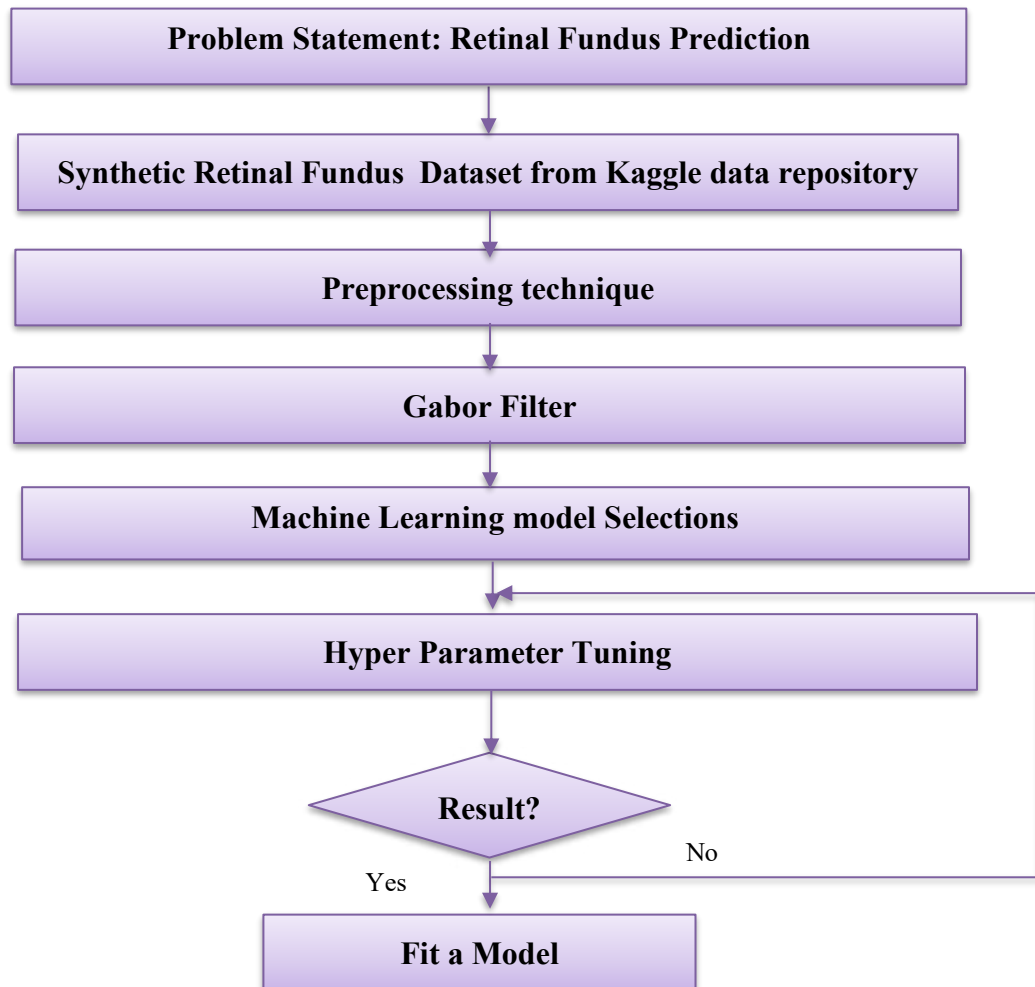


Figure 1: Proposed System

3.4 Performance Evaluation Metrics

- Accuracy: The percentage of right classifications of retinal images over all the images.
- Precision: Number of true positive retinal class predictions divided by actual number of positive predictions made — rate of false positive control.
- Recall (Sensitivity): Fraction of patients with pathological retina who are classified as pathological – the most clinically relevant parameter for the screening for disease.
- ROC Area: Area under the Receiver Operating Characteristic curve — a measure of how well the overall class can be discriminated at any classification value.
- The PRC Area (Area under the Precision-Recall Curve): is measure of the balance of precision and recall profile across thresholds.
- Training Time (seconds): The time to train the classifier model as measured from a wall clock.

IV. EXPERIMENTAL RESULTS

The complete classification result of all the six combinations of the Gaussian filter-based classifiers in algorithms per family are displayed on Table 1 on the synthetic retinal fundus images dataset.

Table 1: Classification Metrics

Category	Classifier	Accuracy	Precision	Recall	ROC	PRC	Time (In Sec)
Instance-Based	GF + Radius Neighbors	82.93	0.82	0.82	0.89	0.86	2.55
Instance-Based	GF + Nearest Centroid	84.92	0.84	0.85	0.91	0.92	4.51
Discriminant	GF + Fisher's Linear Discriminant	80.39	0.79	0.78	0.86	0.84	5.13
Discriminant	GF + Regularized Discriminant	85.29	0.84	0.83	0.91	0.91	2.34
Tree-Based	GF + Decision Tree (CART)	89.18	0.88	0.87	0.95	0.93	5.89
Tree-Based	GF + ID3 Decision Tree	80.35	0.79	0.78	0.86	0.84	5.21

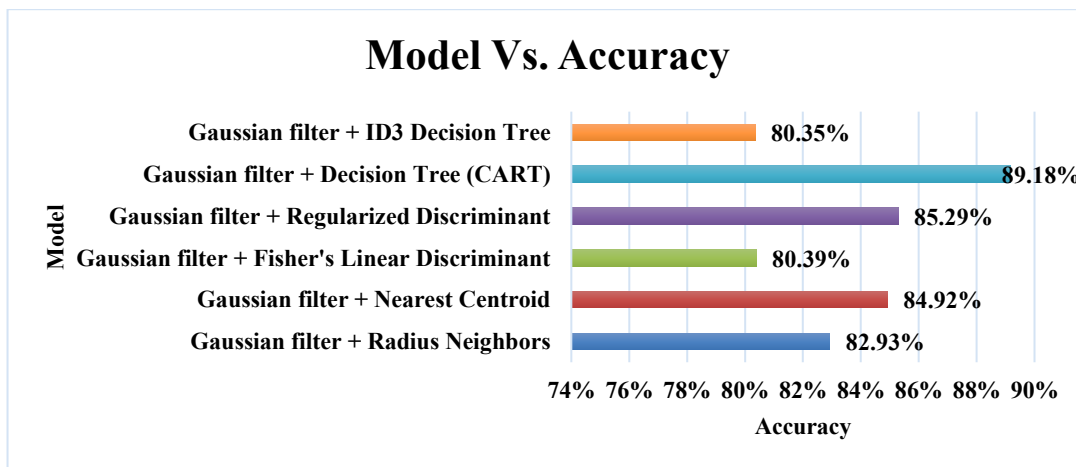


Figure 2: Model Vs Accuracy

The accuracy chart shows a definite three tiered structure corresponding to the three family of classifiers. The best result is offered by the GF+Decision Tree (CART) classifier with 89.18%, where it is the only classifier to top the 88% level with 3.89% margins over the second best (GF+Regularized Discriminant, 85.29%). In the middle tier, there is GF+Nearest Centroid with a score of 84.92%, and GF+Regularized Discriminant with a score of 85.29%. The bottom three (GFR+Radius Neighbors (82.93 %), GF+Fisher's Linear Discriminant (80.39 %), and GF+ID3 Decision Tree (80.35 %)) show that linear discriminant boundaries and entropy splitting of trees are less successful than Gini-criterion CART when applied to Gaussian-filtered retinal features for classification. The overall accuracy of all the classifiers is quite large, 8.83% for a standard synthetic dataset.

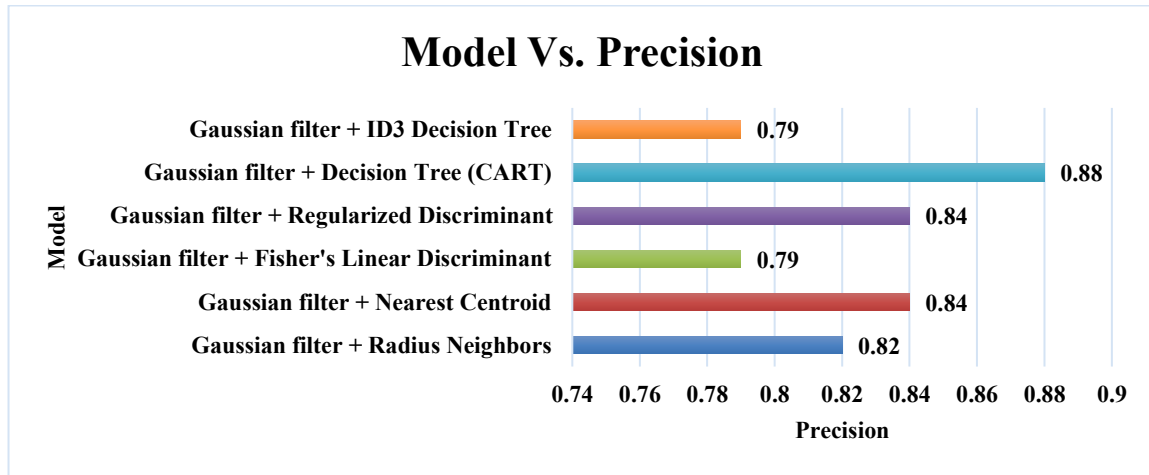


Figure 3: Model Vs Precision

The highest precision of 0.88 is achieved by GF+Decision Tree (CART), indicating that in the experiment, 88% of the time that CART makes a prediction about a retinal pathology class, that prediction is correct (no false positive errors). The second tier consists of GF+Nearest Centroid and GF+Regularized Discriminant (with a precision of 0.84). The lowest precision value, 0.79, is obtained by GF+Fisher's Linear Discriminant (FLD) and GF+ID3, which have a higher false positive classification rate in the Gaussian feature space. The difference in precision between classifiers is 0.09, which is a meaningful difference in the algorithms for delineating retinal class boundaries.

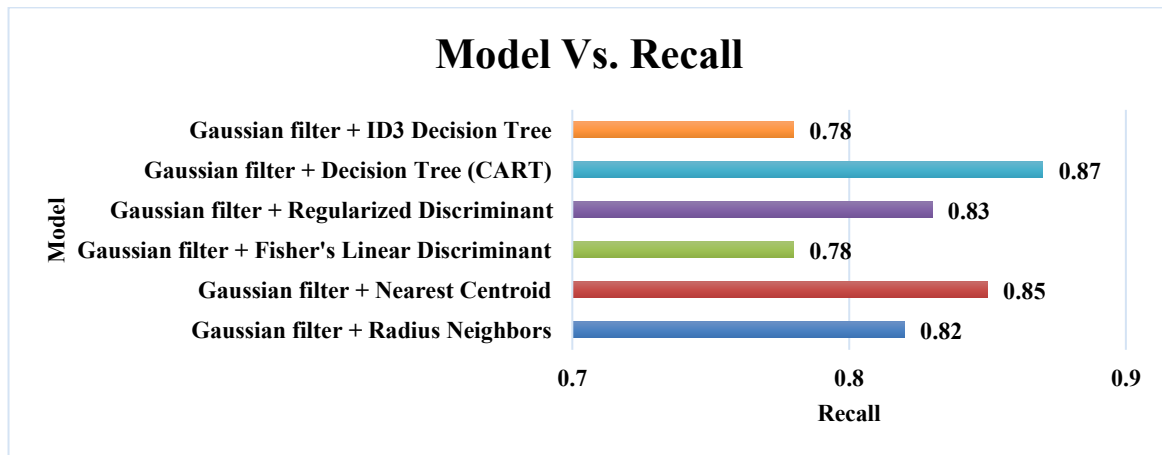


Figure 4: Model Vs Recall

Placing the GF+Decision Tree (CART) at the top with 0.87, it correctly clinically identified 87% of true pathological retinal presentations, the most clinically critical metric for retinal disease screening. Importantly, GF+Nearest Centroid has the second highest recall of 0.85, which is higher than the accuracy of GF+Regularized Discriminant (0.83) despite its lower accuracy, suggesting that it is the most sensitive for the detection of pathology. This is clinically significant: false negative (missed pathology) is a greater clinical threat than false positive in retinal screening, which is dealt with by specialist review [2]. The lowest recall was for GF+Fisher's Linear Discriminant and GF+ID3 both with 0.78.

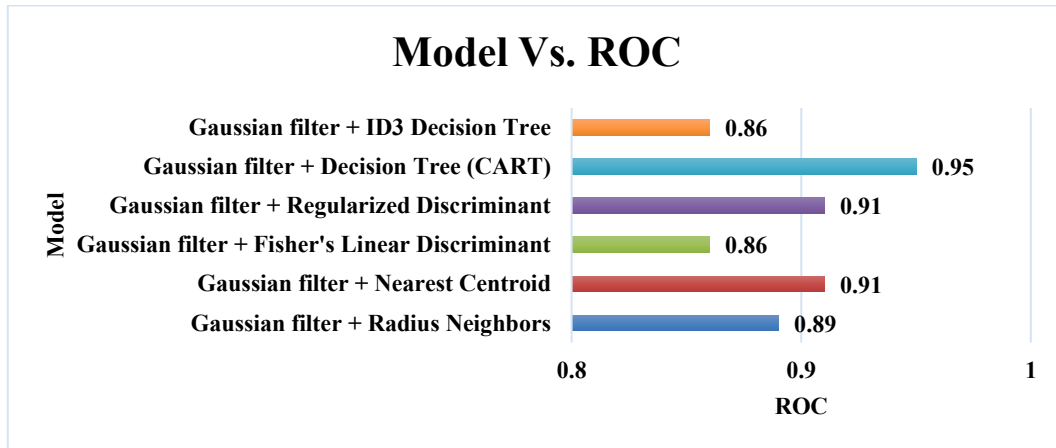


Figure 5: Model Vs ROC

The ROC area chart shows the jini-criterion decision boundaries of the CART to be nearest to the ideal performance curve, with an area of 0.95, the only classification superior to ROC = 0.93, which is the case for the Gaussian-filtered retinal feature space classifiers. Together, GF+Nearest Centroid and GF+Regularized Discriminant have ROC = 0.91; GF+Radius Neighbors has a ROC = 0.89. The non-linear class boundaries of Gaussian retinal features are the least discriminated by linear discriminant projection and entropy-based splitting, as shown by the lowest ROC of 0.86 for both. Specifically, all six classifiers have ROC > 0.86, indicating that the feature representations that are produced by Gaussian filtering are consistently discriminative, independent of the downstream classifier [12].

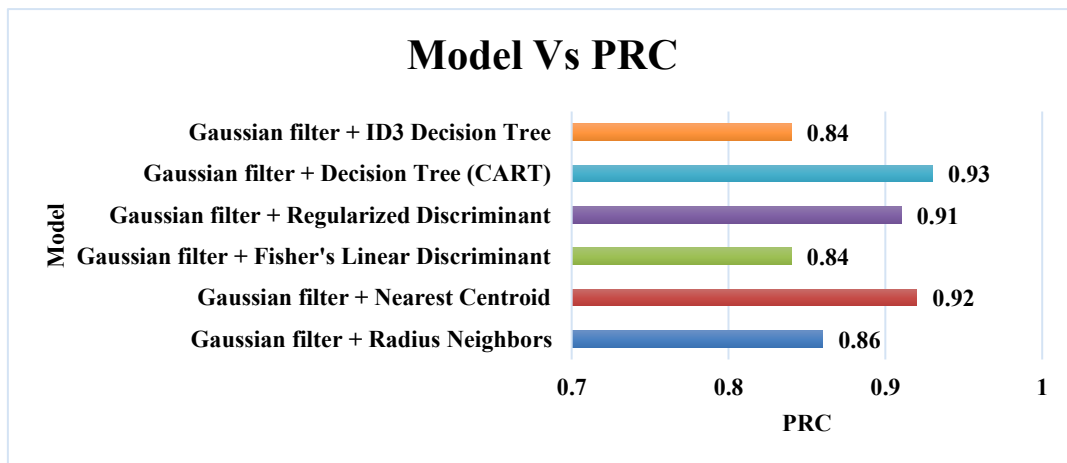


Figure 6: Model Vs PRC

The PRC area chart shows that despite having lower accuracy (84.92% vs 85.29%), GF+Nearest Centroid achieves PRC = 0.92, the second highest among all the experiments for this paper. This indicates that Nearest Centroid adapts the precision-recall tradeoff better at all classification thresholds than Regularized Discriminant — which is the best choice if optimization of classification threshold for screening sensitivity is desired. GF+CART leads at PRC = 0.93. GF+Fisher's Linear Discriminant and GF+ID3 have the lowest PRC of 0.84 (as in all other metrics) [5].

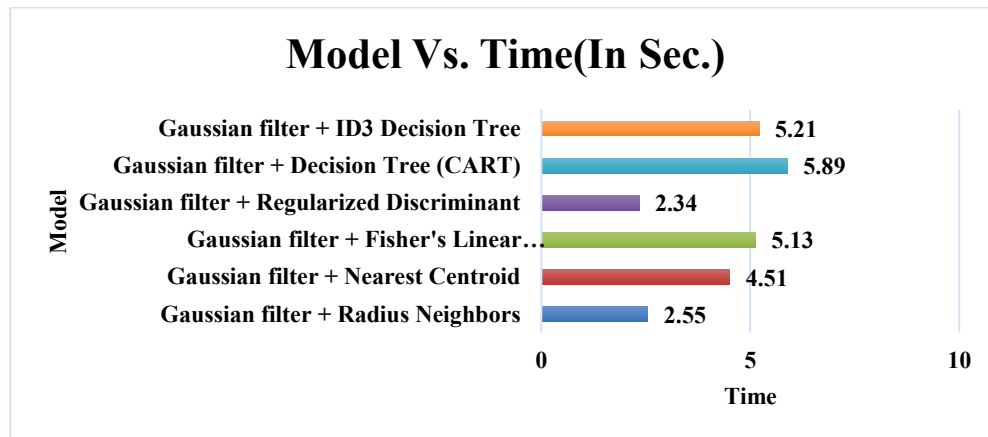


Figure 7: Model Vs Time (In Sec.)

The training time chart shows that GF+Regularized Discriminant is the most efficient of the classifiers in terms of computational time (lowest), with 2.34 seconds, which is the fastest of all classifiers in the experiment, followed by GF+Radius Neighbors at 2.55 seconds. The higher cost group is made up of GF+Fisher's Linear Discriminant (5.13s), GF+ID3 (5.21s), and GF+Decision Tree CART (5.89s) which all take 4.51 seconds or more. Another significant deployment consideration is the fact that at lowest training cost, Regularized Discriminant achieves a competitive accuracy-efficiency balance (85.29% accuracy, ROC 0.91) versus CART (5.89s) with a 2.34s advantage (2.5× speedup).

V. CONCLUSION

In this study, a systematic investigation is carried out on Gaussian Filter based image feature extraction combined with six classifiers belonging to three different algorithmic families, namely instance-based, discriminant and tree-based algorithmic families for automatic classification of synthetic retinal fundus images. Overall, GF+Decision Tree (CART) outperformed all other algorithms tested with the highest accuracy of 89.18, the highest precision of 0.88, the highest recall value of 0.87, the highest ROC area value of 0.95, and PRC area value of 0.93, making CART's Gini criterion decision tree learning the best algorithm available for the Gaussian retinal feature classification under all of these metrics. The configuration with GF+Regularized Discriminant yielded the best computation efficiency (2.34 s), high performance (accuracy 85.29%, ROC 0.91, PRC 0.91), and was also the most deployment-ready configuration for applications with a need for a fast model training time. Non-CART classifiers had recall and PRC values of 0.85 and 0.92, respectively, with GF+Nearest Centroid being the top one for high-sensitivity retinal pathology screening where the main clinical goal is to minimize the number of missed cases [1, 2].

Future research directions include: (i) evaluation of GF feature fusion with other features like Gabor filter responses and GLCM texture features to enrich retinal image representation [6]; (ii) extension to multi-class retinal disease classification including the various grades of DR, stages of glaucoma and different severity levels of AMD; (iii) application of explainable AI techniques to map Gaussian feature importances to specific retinal anatomical regions associated with each disease class; (iv) validation on real clinical retinal fundus datasets to assess generalizability from the synthetic benchmark [3] and (v) comparative benchmarking against deep learning feature extraction pipelines [12,13] on large annotated retinal corpora. In this study, a novel framework for automated classification of retinal fundus images, named GF+CART, is developed which offers a reproducible, computationally efficient and clinically deployable baseline for automated retinal fundus image classification.

REFERENCES

- [1] Lee, R., Wong, T. Y., & Sabanayagam, C. (2015). Epidemiology of diabetic retinopathy, diabetic macular edema, and related vision loss. *Eye and Vision*, 2(1), 17.
- [2] Salz, D. A., & Witkin, A. J. (2015). Imaging in diabetic retinopathy. *Middle East African Journal of Ophthalmology*, 22(2), 145–150.
- [3] Salamat, N., Missen, M. M. S., & Rashid, A. (2019). Diabetic retinopathy techniques in retinal images: a review. *Artificial Intelligence in Medicine*, 97, 168–188.
- [4] Chaturvedi, S. S., Gupta, K., Ninawe, V., & Prasad, P. S. (2019). Advances in computer-aided diagnosis of diabetic retinopathy. *arXiv e-prints*, 1909.09853.
- [5] Saha, S., Xiao, D., Bhuiyan, A., Wong, T. Y., & Kanagasingam, Y. (2019). Color fundus image registration techniques and applications for automated analysis of diabetic retinopathy progression: a review. *Biomedical Signal Processing and Control*, 47, 288–302.
- [6] Biyani, R. S., & Patre, B. M. (2018). Algorithms for red lesion detection in diabetic retinopathy: a review. *Biomedicine and Pharmacotherapy*, 107, 681–688.
- [7] Dashtbozorg, B., et al. (2018). Retinal microaneurysms detection using local convergence index features. *IEEE Transactions on Image Processing*, 27(7), 3300–3315.
- [8] Eftekhari, N., Pourreza, H. R., Masoudi, M., Ghiasishirazi, K., & Saeedi, E. (2019). Microaneurysm detection in fundus images using a two-step convolutional neural network. *Biomedical Engineering Online*, 18(1), 67.
- [9] Zhou, W., Wu, C., Chen, D., Yi, Y., & Du, W. (2017). Automatic microaneurysm detection using the sparse principal component analysis-based unsupervised classification method. *IEEE Access*, 5, 2563–2572.
- [10] Wu, B., Zhu, W., Shi, F., Zhu, S., & Chen, X. (2017). Automatic detection of microaneurysms in retinal fundus images. *Computerized Medical Imaging and Graphics*, 55, 106–112.
- [11] Wang, S., Tang, H. L., Turk, L. A., Hu, Y., Sanei, S., Saleh, G. M., & Peto, T. (2017). Localizing microaneurysms in fundus images through singular spectrum analysis. *IEEE Transactions on Biomedical Engineering*, 64(5), 990–1002.
- [12] Budak, U., Sengur, A., Guo, Y., & Akbulut, Y. (2017). A novel microaneurysms detection approach based on convolutional neural networks with reinforcement sample learning algorithm. *Health Information Science and Systems*, 5(1), 14.
- [13] Habib, M. M., et al. (2017). Detection of microaneurysms in retinal images using an ensemble classifier. *Informatics in Medicine Unlocked*, 9, 44–57.
- [14] Derwin, D. J., Selvi, S. T., & Singh, O. J. (2019). Secondary observer system for detection of microaneurysms in fundus images using texture descriptors. *Journal of Digital Imaging*, 33(1), 159–167.
- [15] Mayya, V., Sowmya Kamath, S., & Kulkarni, U. (2021). Automated microaneurysms detection for early diagnosis of diabetic retinopathy: a comprehensive review. *Computer Methods and Programs in Biomedicine Update*, 1, 100013.
- [16] <https://www.kaggle.com/datasets/taanii/synthetic-retinal-fundus-images>



INTERNATIONAL
STANDARD
SERIAL
NUMBER
INDIA



INTERNATIONAL JOURNAL OF INNOVATIVE RESEARCH

IN SCIENCE | ENGINEERING | TECHNOLOGY

 9940 572 462  6381 907 438  ijirset@gmail.com



www.ijirset.com

Scan to save the contact details